Radiocarbon, Vol 62, Nr 3, 2020, p 601–615 DOI:10.1017/RDC.2020.35
Selected Papers from the Mortar Dating International Meeting, Pessac, France, 25–27 Oct. 2018

RADIOCARBON DATING OF DOLOMITIC MORTARS FROM THE CONVENT SAINT JOHN, MÜSTAIR (SWITZERLAND): FIRST RESULTS

Marta Caroselli[1]* • Irka Hajdas[2] • Patrick Cassitti[3]

[1]University of Applied Arts and Sciences of Southern Switzerland (SUPSI), Institute of Materials and Construction (IMC), Switzerland
[2]ETH, Laboratory of Ion Beam Physics, Zurich, Switzerland
[3]Foundation Pro-Kloister Müstair (FM), Switzerland

ABSTRACT. The monastery of St. John in Müstair, a UNESCO world heritage site, preserves archaeological remains and stone structures dated from the 8th century to the present. It has been extensively studied archaeologically so that numerous samples of historical materials, including mortar, are available for study. In addition to that, some of the structures have been precisely dated with dendrochronology. The monastery is located in a region characterized by dolomite rocks and the mortars are therefore of dolomitic nature, being perfectly suited to test the possibility of being dated with ^{14}C. Furthermore, the presence of embedded carbon fragments has provided additional independent data to support or deny the results of mortar dating. A comparison of the results obtained from radiocarbon (^{14}C) dating of bulk mortars, sieved fractions enriched in binder, lime lumps and carbon fragments, for two samples is presented, in relation to the petrographic characterization and the mineralogical phase content. This preliminary study shows that the dating of ^{14}C can potentially be applied to the mortar of Müstair, as results in accordance with the established chronologies have been obtained for one sample. However, if the dolomitic sand contamination is very high, further studies are needed to develop a specific sample preparation technique.

KEYWORDS: dolomite, mortar, radiocarbon dating.

INTRODUCTION

Within the framework of the project "Mortar technology and construction history at Müstair Monastery"[1], a selection from about 5000 mortar samples ranging from the 8th to the 20th century, collected in over 30 years of archaeological excavations on site, has been studied in detail. Such quality and number of samples is very rare and provides a unique opportunity for further analytical studies. Absolute dating of mortars is crucial to date the construction phases of archaeological sites and to confirm or challenge existing chronologies. The method of selective dissolution showed promising results in dating Roman and medieval mortars (Hajdas et al. 2012). Furthermore, an attempt to systematically test the possibility of dating mortars with various compositions was carried out by comparing methods and laboratories within the mortar dating intercomparison study (Hajdas et al. 2017). But the wider variety of mineralogical phases in a dolomitic mortar, due to the more complicated model of the dolomitic lime cycle, were identified as a potential source of error for the dating process (Michalska et al. 2017). The alpine region around the monastery is characterized by dolomitic rock formations and the mortars used at Müstair are of a dolomitic nature (Cavallo et al. 2019), giving the possibility to test their potential to be dated with ^{14}C.

Dolomite $CaMg(CO_3)_2$ is a calcium and magnesium carbonate that is formed through the substitution by Mg atoms in the structure of calcium carbonate ($CaCO_3$). This process does not always occur completely and, as a result, dolomite limestones can contain variable amounts of dolomite (Warren 2000). During the burning process of dolomite limestone, in addition to calcium carbonate, magnesium carbonate ($MgCO_3$) decomposes, with the formation of magnesium oxide (MgO). The calcination of dolomite limestone happens between 510°C and 750°C and it is necessary not to exceed these temperatures to avoid the

*Corresponding author. Email: marta.caroselli@supsi.ch.
[1]Funded by the Swiss National Fund (SNSF), the Foundation Pro Monastery of St. John and the Biosfera Val Müstair. http://www.supsi.ch/imc/istituto/progetti/dettaglio.5797.backLink.76c387dc-d6bb-47ae-8c06-3b4678190667.html.

formation of sintered magnesium oxides, which have a very slow reactivity. Furthermore, due to the very low solubility in water of magnesium hydroxide ($Mg(OH)_2$) its carbonation is very slow and often incomplete. The formation of magnesite is therefore often slower than calcite, while that of hydroxy-carbonates of magnesium (such as artinite, hydromagnesite, etc.) is favored (Diekamp et al. 2009). The slow carbonation of these mortars can cause a delay in the absorption of CO_2 and result in an incorrect outcome of the age with radiocarbon (^{14}C).

In particular, the objectives of this paper are the following:

1. To verify if the ^{14}C dating can be applied to mortar made by dolomitic raw material, a verification which is possible because the age of the main church was clearly established by dendrochronology (Wacker et al. 2014);
2. To understand which type of sample preparation is suitable for dating dolomitic mortar, as in other studies lime lumps and bulk mortars showed different ^{14}C contamination and they are highly complementary for a reliable mortar dating (Lindroos et al. 2018);
3. To investigate if the construction phases of the monastery can be chronologically distinguished with mortar dating.

The first results obtained by ^{14}C dating of mortars belonging to the first Carolingian phase are presented and discussed in relation to their petrographic and mineralogical characterization. Once the potential feasibility of the dolomitic mortar dating is demonstrated, the method would be applied to investigate controversial building phases of the monastery, for which no well-established dating options are available.

Description of the Case Study

The monastery complex of St. John in Müstair is an outstanding example of Carolingian art and architecture. It is located in the Eastern Alps, in the Vinschgau/Val Venosta region which is known for its many early medieval and Romanesque churches. The region was of strategic importance at least since Roman times because of its mountain passes, which allowed a safe crossing of the main alpine divide (Figure 1). The via Claudia Augusta, built by the Romans after the conquest of Raetia in the late 1st century BC, remained one of the most important north-south routes through the Alps well into the early modern period (Grabherr 2006). From the 6th century onward the area came under the influence of the Merovingian and Frankish rulers, who had to contend with the neighboring Lombards to the south and Bavarians to the east. In 774 Charlemagne conquered the Lombard Kingdom. This bestowed even greater strategic importance to the alpine passes in the Val Müstair and Vinschgau/Val Venosta region.

It is within this historical and political context that the monastery of St. John was built. The size of the first Carolingian monastery, as known from archaeological excavations (Sennhauser 1996), is monumental, and comparable to other large monasteries of the time, such as the monastery of Reichenau, on Lake Constance, SW-Germany (Zettler 1988), or San Vincenzo al Volturno, in the Molise region of central Italy (Hodges 1993). It possessed two sacred buildings, the monastery church, which is a three apse aisleless church with two annexes to the north and south, both with their own apse and connected to the nave by large arches, and the Holy Cross chapel, with a trefoil-shaped layout, an upper floor and a lower floor used as crypt (Figure 2). The monastery church and the Holy Cross chapel were decorated

https://doi.org/10.1017/RDC.2020.35 Published online by Cambridge University Press

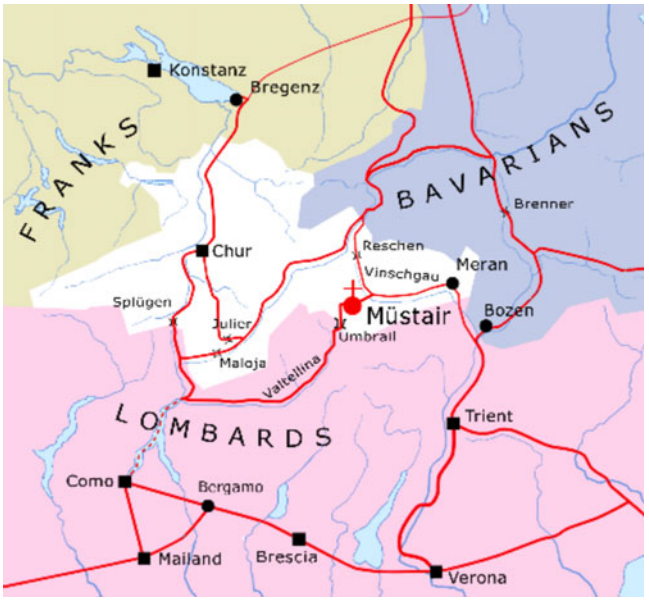

Figure 1 The territory of Raetia Curiensis in the second half of the 8th century with the main roads and mountain passes; see Goll et al. (2007, with modifications).

with mural paintings and sculpted marble choir screens. The Holy Cross chapel was also provided with rich stucco decoration.

Both sacred buildings are still standing and in use today. Their construction date can be precisely determined by dendrochronology. A wooden beam preserved in the eastern gable of the monastery church was felled in the winter of 775/6 AD, while the wooden beams and planks used for the construction of the ceiling of the Holy Cross chapel, which are to a large part still in place and in use today, were felled between 784/5 and 788/9 (Hurni et al. 2007). In the medieval period, timber for the construction of buildings was usually felled in winter and processed in the following months (Descoeudres 2007). This means that the construction of the church was probably completed in 776, and that work on the Holy Cross chapel probably ended in 789 or shortly after. The remaining convent buildings, which are not preserved above ground and therefore did not yield any dendrochronological date, were most likely built in between these dates.

Sometimes after the completion of the first Carolingian monastery, the so-called "loggia building" was added to the southern tract (Figure 2C). The monastery remained in use throughout the centuries up to the present time. It was never completely rebuilt, but buildings were continually replaced or added to the site, so that today it features architectural and archaeological remains from 12 centuries of European history. This makes it an ideal site for studying and testing mortar dating methods.

MATERIAL AND METHODS

The choice of the first two samples (Table 1) to be used as a test for mortar dating was made considering the results of the petrographic characterization of 52 Carolingian samples. Within

https://doi.org/10.1017/RDC.2020.35 Published online by Cambridge University Press

Table 1 Description of samples used for dating. ff = binder fine fraction, LL = lime lumps.

Sample ID	Provenance/group	Bulk fraction	Lime lumps	Charcoal
6577	Main church/group 1	45–63 µm (ff) 63–75 µm (ff)	Lime lump 1 (LL1) Lime lump 2 (LL2)	1 fragment (CH)
957	Courtyard/group 2	45–63 µm (ff) 63–75 µm (ff)	Lime lump 1 (LL1) Lime lump 2 (LL2)	Not available

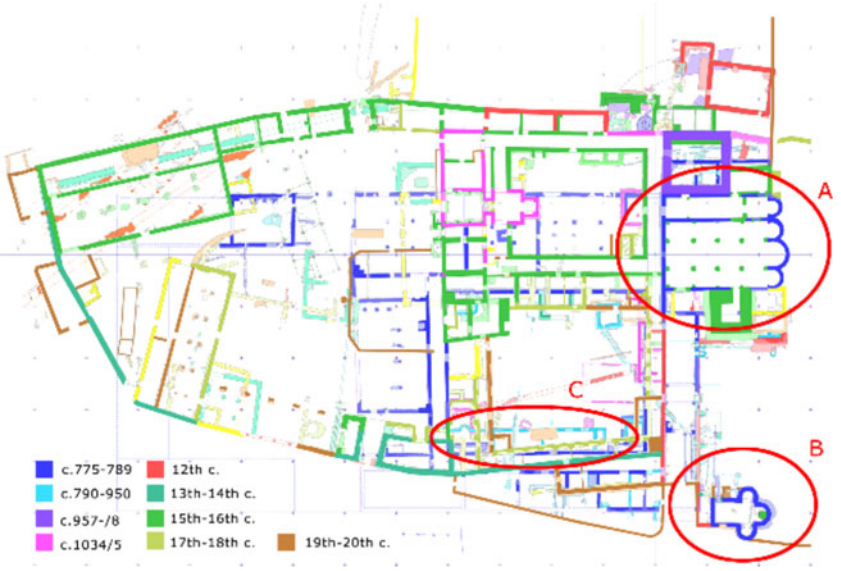

Figure 2 Archaeological phase plan of the monastery of St. John: (A) Monastery church; (B) Holy Cross chapel; (C) Loggia building (cyan). Sennhauser and Courvoisier (1996) with modifications.

this group of samples two different groups of bedding mortar have been identified with different petrographic characteristics: one group comes from the main church and one from the large adjacent building complex to the west, which consists of the convent and the Holy Cross chapel (Caroselli et al. 2019). Furthermore, high presence of lime lumps has been considered as an important element for the selection of a sample. An embedded charcoal fragment in one sample has been extracted and dated to obtain independent data necessary to support or contrast the results of the dating of the mortar binder.

Polished thin sections were prepared by a specialized laboratory. Polarized light microscopy (PLM) on the thin sections was carried out for mineralogical and textural analysis; a Zeiss Axioskop 4.0 Polarizing Light Microscope (PLM) was used and micrographs were acquired with a digital camera, and processed with the software Axiovision (Zeiss, release 4.5.1). The following interesting features for mortar dating were observed: binder (structure, color, birefringence, homogeneity), lime lumps (types, internal structures, quantity and size), aggregate grains (grain sizes, mineral and rock types present, estimation of the grain size distribution), additions (brick grains or organic material), macro-porosity and especially secondary calcite or hydromagnesite fillings of voids.

https://doi.org/10.1017/RDC.2020.35 Published online by Cambridge University Press

The binder enriched fraction of the two samples was extracted by dry sieving. The samples were broken avoiding fine splinters of aggregates. The crushed material was vibrated in a sieve series. The fine grain-size fraction (ff) 45–63 μm and the fraction 63–75 μm were homogenized and divided in two parts: one part was analyzed by X-ray powder diffraction (XRPD) and the other was used for mortar dating. Lime lumps (LL) were mechanically separated from the mortar bulk under the stereomicroscope.

The mineralogical analyses of the mortar binders were carried out using XRPD. After grinding in an agate mortar, randomly oriented samples were prepared and deposited in the hollow of a Si monocrystal zero background plate, supplied by Assing spa, Monterotondo, Italy. A Rigaku Miniflex system, operating in θ:2θ mode was used; generator setting 30 kV, 10 mA, Cu anode (Cu Kα -1.5418 Å), Ni filter, 2 θ range 5–55°, step size 0.02°, scan speed 0.3° min^{-1}. Qualitative phase determination was carried out using the software QualX2.0 (Altomare et al. 2015) and the correlated COD database (Gražulis et al. 2009).

Sequential Dissolution Method for ^{14}C Dating of Mortar

The method of sequential dissolution targets the fast-dissolving component of the binder. The procedure follows the method described in detail by Hajdas et al. (2020 in this issue). The sieved mortar fraction of grain size 45–63 μm and lime lumps were used. Prior to the sequential procedure the whole samples (bulk) was dissolved in acid and graphitized for the AMS analysis. This step was to estimate carbon content of each sample as well as to measure the range of the ages of the carbonates. Measurement of bulk is considered exploratory although, dependent on the type of mortar, this fraction has a potential of providing the accurate ages.

For sequential dissolution, subsamples containing ca. 50 mg of the mortar powder fraction were placed in one of the chambers of the special dual chamber glass vessel. The second chamber has been filled with 10 mL of concentrated phosphoric acid (85% H_3PO_4). The vessel was then closed and evacuated at room temperature, prior to pouring of acid to the chamber, which contained mortar. This process was timed and freezing of purified (passing through a water trap) CO_2 in liquid nitrogen (LN) was performed in sequence: 4 consecutive fractions were collected after each 3 s. Carbon content of each collected fraction was measured and 10–100 μg of C was trapped in a 4 mm tube to be flame sealed for analysis using Gas Ion Source (GIS) AMS facility at ETHZ (Ruff et al. 2010). Graphite samples were also measured using the MICADAS at ETH Zurich (Synal et al. 2007). Solid and gas formed samples were analyzed together with corresponding size of standard (OXA II) and background samples (C-1, IAEA).

RESULTS

Petrographic Analyses

The binder of sample 6577, which was taken from the western wall of the monastery church (Figure 2), shows heterogeneous clear and dark beige color with radial dark spots, under the microscope. In this mortar, lime lumps *sensu strictu*, underburned and overburned fragments (Elsen 2006) can be distinguished, the last two being potentially source of error for mortar dating (Lubritto et al. 2015). The aggregate grain size is prevalently medium and coarse,

https://doi.org/10.1017/RDC.2020.35 Published online by Cambridge University Press

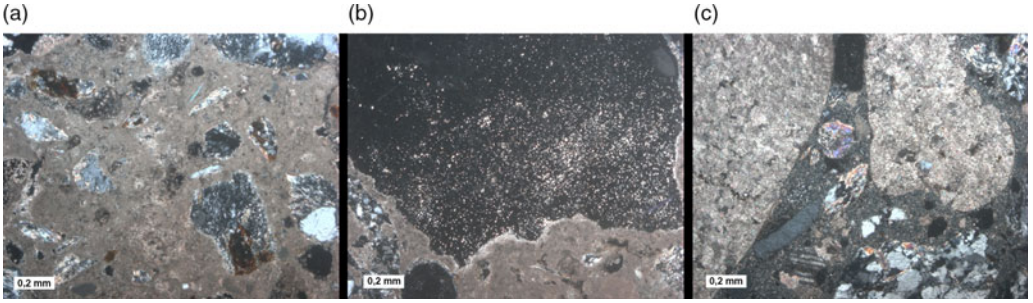

Figure 3 Thin section images 5×, XPOL: (a) Sample 6577 bedding mortar of the church; the aggregate of this mortar is mainly of metamorphic siliceous composition; (b) same sample of A, here a big overburned BRP is shown with a glassy structure and the neoformation of tiny calcite crystals; (c) sample 957 bedding mortar of the courtyard with big dolomite crystals as aggregate.

not well selected. The composition is: rock fragments of gneiss, rich in quartz and feldspar, schists and micas (muscovite and chlorite). The absence of carbonate minerals (neither dolomite nor calcite) avoids the potential harmfulness of dead carbon contamination from the aggregate (Figure 3A), but the contribution of the binder related particles (BRP) left in the binder which during the production process did not completely lose former CO_2, and therefore still containing dead carbon, should be targeted. Indeed, in this particular mortar a relevant presence of overburned BRP is observed, showing the typical glassy structure and texture, as well as the neoformation of tiny calcite crystals (Figure 3B).

The sample 957 is a wall mortar coming from the buildings on the western side of the Carolingian courtyard (Figure 2). The binder is homogeneous, with a clear beige color. The lime lumps are frequent and dark phases can be observed within them. The grain size of the aggregate varies from very fine to medium-coarse, not sorted. The aggregate is composed by fragments of gneiss, schists, quartz, feldspar, dolomite, limestone, calcite and micas (Figure 3C). In this mortar the potential source of dead carbon is the relevant presence of diverse carbonate sand (Caroselli et al. 2019).

XRPD Analysis Results

Qualitative mineralogical analysis of the sieved fraction 43–63 μm of the samples is reported in Table 2. Results indicate that the binder of the samples 6577 is dolomitic due to the presence of hydromagnesite. The presence of phyllosilicate minerals, quartz and dolomite in both samples is due to the fraction of aggregates that has passed the 63 μm sieve.

Mortar Dating Results

Results of ^{14}C dating are summarized in Table 3. The measured ^{14}C content of mortar ($F^{14}C$) and corresponding ^{14}C ages of different fractions which were calculated following Stuiver and Polach (1977) are listed along with the weight of the carbon that was released in each fraction. AMS allows for measurement of $\partial^{13}C$ however the fractionation in the process of the sequential dissolution is possibly changing the original isotopic signal of the specific mortar fraction (Folk and Valastro 1976).

https://doi.org/10.1017/RDC.2020.35 Published online by Cambridge University Press

Table 2 XRPD results. Cal = calcite, Qz = quartz, Dol = dolomite, Ilt/Ms = illite/muscovite, HMgs = Hydromagnesite.

	Qualitative mineralogical analysis				
ID	Cal	Qz	Dol	Ilt/Ms	(H)Mgs
6577	+	+	–	+	tr
957	+	+	+	+	–

Table 3 Results of AMS ^{14}C analysis. Sample description gives information about the grain size used. Fraction defines the collection time and the technique of AMS measurement. GIS stands for gas ion source, graphite for solid samples. $F^{14}C$ is the measured ^{14}C content and the ^{14}C ages are calculated based on this value. The amount of carbon released and measured in the samples is given as mg of C. ff= binder fine fraction, LL= lime lumps.

Lab code	Sample	Fraction	$F^{14}C$	±1σ	^{14}C age (BP)	±1σ	$\delta^{13}C$ (‰)	mg C
ETH-88628	957ff, 45–63 µm	1–3 s, GIS	0.857	0.005	1237	47	–42.2	0.08
		1–3 s, GIS	0.853	0.005	1274	47	–46.1	0.08
		4–6 s, GIS	0.852	0.005	1290	46	–36.3	0.09
		7–9 s, GIS	0.840	0.006	1402	61	–28.3	0.08
		10–12 s, GIS	0.847	0.006	1334	60	–31.4	0.08
ETH-88628	957ff, 45–63µm	1–3 s, GIS	0.844	0.006	1360	58	–28.6	0.09
		1–3 s,GIS	0.842	0.006	1384	56	–29.7	0.08
		4–6 s, GIS	0.850	0.006	1306	52	–23.2	0.09
		7–9 s, GIS	0.848	0.006	1324	61	–24.7	0.09
		10–12 s, GIS	0.840	0.006	1398	62	–19.6	0.08
ETH-88628	957ff, 45–63µm	Bulk, graphite	0.725	0.002	2585	24	–18.0	0.64
ETH-88629	957_LL1	1–3 s, GIS	0.862	0.005	1192	49	–16.7	0.07
		1–3 s, GIS	0.863	0.005	1180	47	–18.6	0.07
		4–6 s, GIS	0.868	0.005	1137	46	–12.5	0.08
		7–9 s, GIS	0.861	0.006	1198	60	–12.9	0.08
		10–12 s, GIS	0.862	0.007	1195	62	–14.1	0.06
ETH-88629	957_LL1	Bulk, graphite	0.857	0.002	1240	22	–11.4	0.86
ETH-88630	957_LL2	1–3 s, GIS	0.845	0.005	1351	49	–36.2	0.10
		1–3 s,GIS	0.840	0.006	1402	62	–35.9	0.08
		4–6 s, GIS	0.851	0.005	1298	47	–37.0	0.08
		7–9 s, GIS	0.845	0.006	1351	61	–34.9	0.08
		10–12 s, GIS	0.848	0.006	1325	61	–21.4	0.04
ETH-88630	957_LL2	Bulk, graphite	0.847	0.002	1334	22	–24.2	0.98
ETH-88631	6577ff, 45–63µm	1–3 s, GIS	No result				0.0	0.03
		4–6 s, GIS	0.863	0.007	1181	62	–16.4	0.02
		7–9 s, GIS	0.863	0.005	1184	46	–32.9	0.07
		10–12 s, GIS	0.864	0.006	1173	60	–33.1	0.08
		Bulk, graphite	0.846	0.003	1341	29	–19.9	0.24
ETH-88632	6577_LL1	Bulk, graphite	0.891	0.003	923	25	–22.4	0.39
ETH-88633	6577_LL2	4–6 s, GIS	0.916	0.008	702	67	–0.3	0.04
		7–9 s, GIS	0.900	0.005	843	45	–13.0	0.05
		10–12 s, GIS	0.898	0.006	867	57	–4.8	0.10
		Bulk, graphite	0.892	0.002	916	22	–6.9	0.87
ETH-88634	6577_CH	Charcoal	0.848	0.002	1331	21	–26.5	1.0
ETH-89538	957ff, 63–75µm	Bulk, graphite	0.748	0.002	2337	23	–19.4	0.79
ETH-89539	6577ff, 63–75µm	Bulk, graphite	0.861	0.003	1200	30	–22.8	0.27

https://doi.org/10.1017/RDC.2020.35 Published online by Cambridge University Press

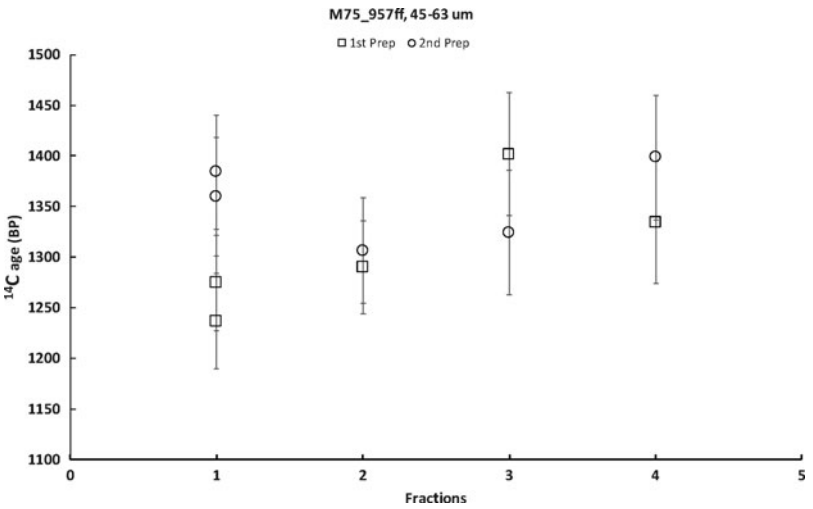

Figure 4 Results of sequential dissolution from 2 independent preparations. In both preparations the fast fractions#1 (1–3 s) resulted in sufficient amount of CO_2 for duplicate GIS measurements. Result of measurement on the bulk is not shown as it is out of scale: 2585 ± 24 BP. ff= binder fine fraction.

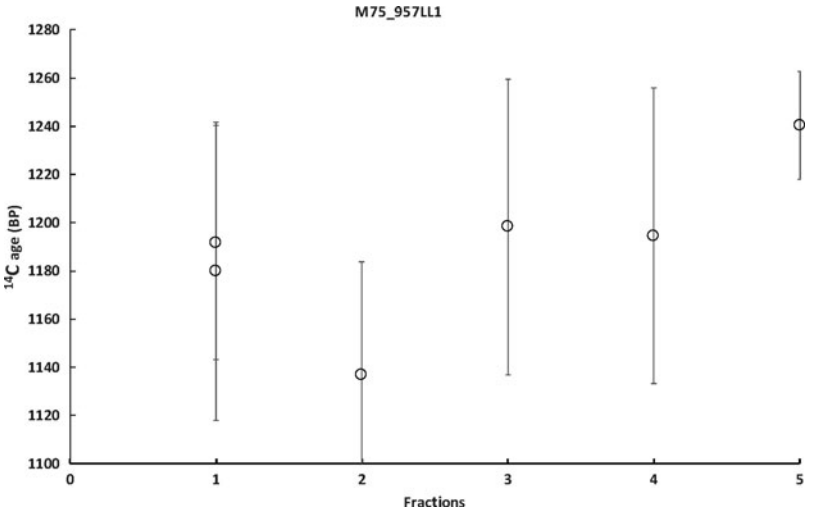

Figure 5 Results of sequential dissolution. The fast fractions#1 (1–3 s) resulted in sufficient amount of CO_2 for duplicate GIS measurements. Result of measurement on the bulk is shown as the fraction #5. LL= lime lumps.

Figures 4–7 allow the assessment of the method of removing the old (geological) component that is assumed to dissolve at lower speed (Lindroos et al. 2007). The presence of such a component, which is an indicator of contamination with geological material, can be quickly assessed by comparison of the ages of the fractions.

Calibration of the evaluated final ages was performed using OxCal 4.2 (Ramsey and Lee 2013) with the INTCAL13 dataset (Reimer et al. 2013). Calibrated ages are summarized in Table 3 and shown in Figures 4–7.

https://doi.org/10.1017/RDC.2020.35 Published online by Cambridge University Press

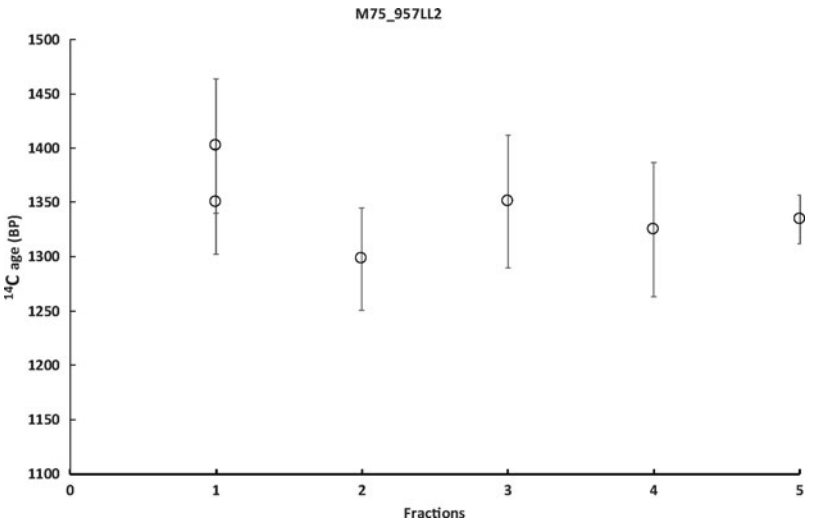

Figure 6 Results of sequential dissolution. The fast fractions#1 (1–3 s) resulted in sufficient amount of CO_2 for duplicate GIS measurements. Result of measurement on the bulk is shown as the fraction #5. LL= lime lumps.

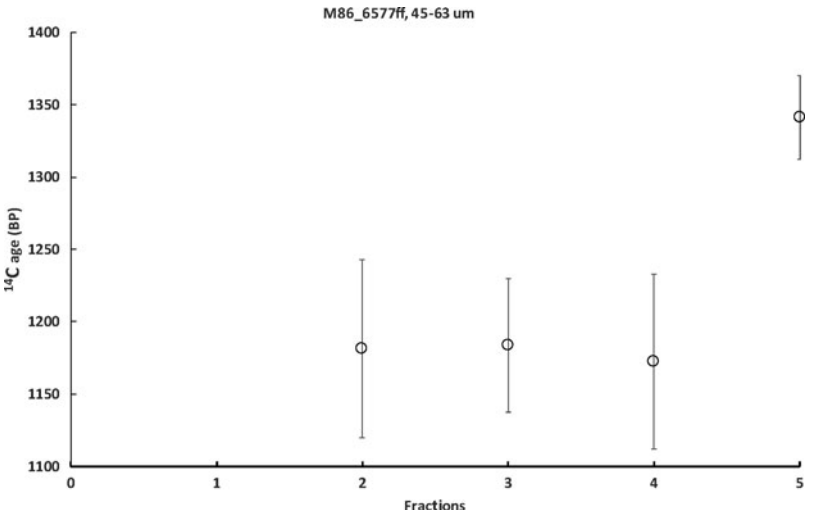

Figure 7 Results of sequential dissolution. The fast fractions#1 (1–3 s) resulted in an insufficient amount of CO_2 even for GIS measurement. Result of measurement on the bulk is shown as the fraction #5. ff= binder fine fraction.

The principle of ^{14}C dating of mortar using sequential dissolution relies on the separation of carbon from the fast-dissolving component. In the ideal case of mortar samples free of contamination (old and young) the ^{14}C ages of all the fractions are in agreement, or forming an age-plateau (Heinemeier et al. 2010). Although such distribution is rather unusual, an assessment of reliability of ^{14}C ages is based on the distribution of ^{14}C ages of fractions in sequence. The first fraction is considered to be the best estimated of the ^{14}C

https://doi.org/10.1017/RDC.2020.35 Published online by Cambridge University Press

and if followed by an agreement with the 2nd fraction, such ^{14}C age can be considered the most accurate measure of the moment when the binding reaction occurred.

In this case, each of the samples tested presents a somewhat different picture. The ^{14}C ages of bulk samples (fraction #5 in Figures 4–7) are very helpful for evaluating the sequence development and effectiveness of the method. In the case of sample 957ff, 45–63 μm, the age of bulk 2585 ± 24 BP is more than 1000 years older than the first fraction. A repeated sequential dissolution resulted in an agreement between the results of the 1st and 2nd preparations. This result means that bulk mortars were highly contaminated with dead carbon and that after sequential dissolution treatment a part of the contamination has been eliminated. The ^{14}C age of the sample 957 is based on a mean value of ages of 1st fractions from 2 preparations (Table 4, Figure 4).

The samples lime lumps LL1 and LL2 from the sample 957 were also treated with sequential dissolution. The results show slight difference between the lime lumps, but all 3 samples result in a coherent age interval between 650 and 880 CE (Figure 8).

The Sample 6577ff, 45–63 μm was prepared and analyzed only once and the first (1–3 s) dissolution fraction was too small even for GIS analysis. However, the ages of all the 3 following fractions were so coherent that the ages were combined and calibrated resulting in 1180 ± 32 BP and calendar age of 729–961 CE. This is a little younger than the age of the whole bulk of this sample 1341 ± 29 BP and charcoal 1331 ± 21 BP, both calibrated fall into the interval 644–765 CE (Table 4 and Figure 9).

The ^{14}C ages obtained for 6577_LL2 were not calibrated as the ages appear to be significantly younger than the charcoal and the bulk fraction discussed above.

Results of ^{14}C dating bulk (no sequential solution) of the remaining samples are a primary assessment of the samples for future analysis. Samples 957ff, 63–75 μm and 6577ff, 63–75 μm were analyzed to see how the different grain sizes relate to the isotopic composition of the 45–63 μm fraction. It appears that the 6577ff, 63–75 μm has the same ^{14}C age as the 45–63 μm fraction i.e. 1200 ± 30 BP.

DISCUSSION

In the sample belonging to the main church 6577 characterized by mostly quartz and feldspar sand and without dolomite mineral, the dating has provided results consistent with the dendrochronological dating (Hurni 2007). The charcoal sample was a little older than the mortar and this is also consistent. The bulk mortar turned out to be older and this is consistent with a slight contamination that could be due to small fractions of carbonate sand, whose presence cannot be excluded, and/or fragments of BRP that did not completely react during the burning process. The ^{14}C ages obtained for the lump of this mortar 6577_LL2 were significantly younger and thus they were not calibrated. This result can be explained by the presence of the overburned lumps, in which secondary calcite formed in more recent times can be observed (Figure 3B). The presence of delayed carbonation reaction of some lumps can also not be excluded.

On the contrary, in the sample of the courtyard 957, in which the presence of dolomitic sand is abundant, this component was not completely separated with the sequential dissolution, providing data in agreement with each other but discordant with the dendrochronology

https://doi.org/10.1017/RDC.2020.35 Published online by Cambridge University Press

Table 4 Combined and calibrated ages (95.4% confidence level) obtained using OxCal v.4.2 calibration program (Ramsey and Lee 2013) with IntCal data set (Reimer et al. 2013). ff = binder fine fraction, LL = lime lumps. In the last column the dendrochronology results obtained from the church according to Hurni et al. (2007: 111, Table 4) were included for comparison.

Lab code	Description	^{14}C age ±1σ (BP)	Range cal years (CE)	Comment	Dendro date
ETH-88628	R_Combine 957ff, 45–63 µm	1304 ± 26	660–769	χ^2 test: df=3 T=5.4 (5% 7.8)	—
ETH-88629	R_Combine 957_LL1	1224 ± 19	696–883	χ^2 test: df=2 T=1.8 (5% 6.0)	—
ETH-88630	R_Combine 957_LL2	1337 ± 17	650–760	χ^2 test: df=5 T=2.0 (5% 11.1)	—
ETH-88631	R_Combine 6577ff, 45–63 µm	1180 ± 32	729–961	χ^2 test: df=2 T=0.0 (5% 6.0)	775/776
ETH-88631	R_Date 6577ff_45–63 µm _BULK,	1341 ± 29	644–765	Calibrated	775/776
ETH-88634	R_Date 6577_CH	1331 ± 21	651–764	Calibrated	775/776

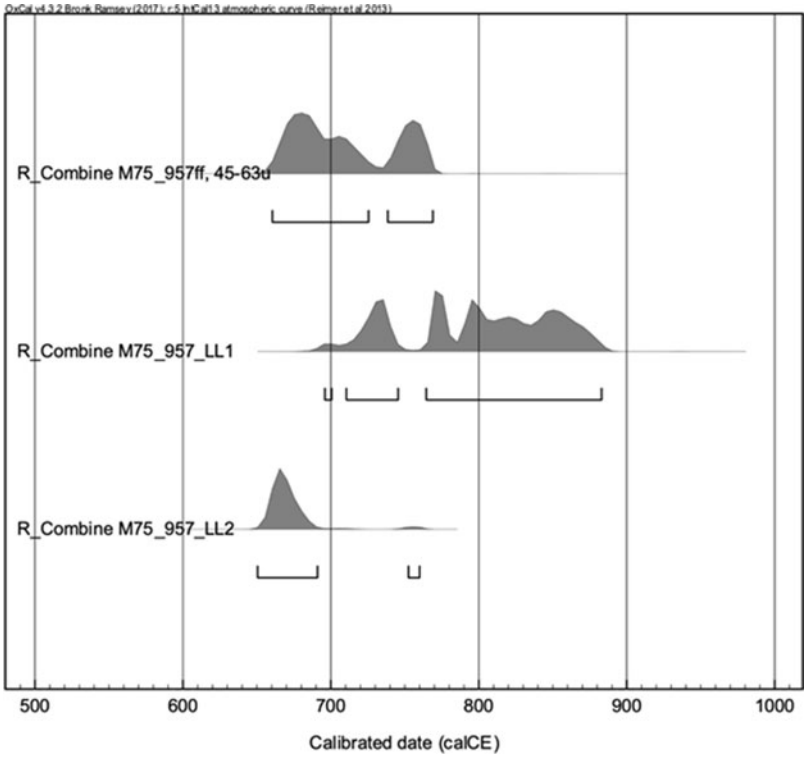

Figure 8 Calibrated ^{14}C age of the sample 957 sieved fraction (ff) 45–63 and the lime lumps LL1 and LL2. The results show slight difference between the lime lumps but all 3 samples result in a coherent age interval between 650 and 880 CE (Table 4). ff = binder fine fraction, LL = lime lumps.

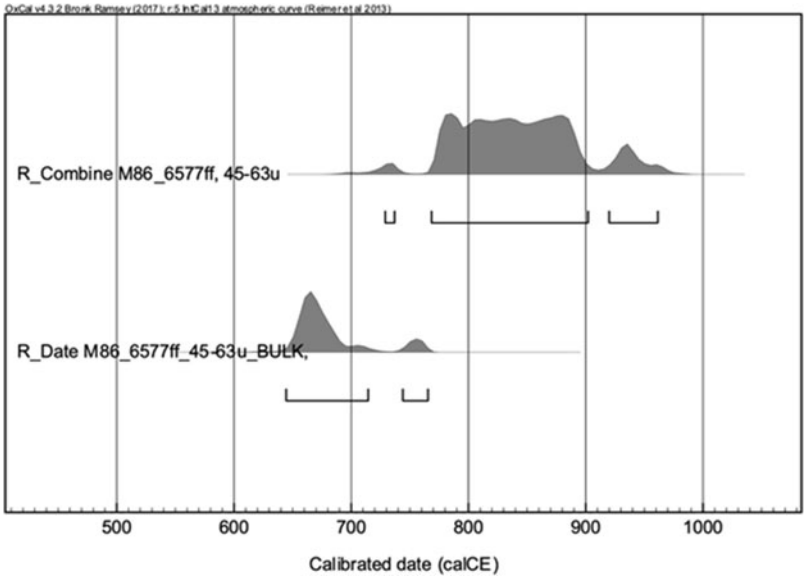

Figure 9 Calibrated age of the sample 6577ff, 45–63 μm (fractions 2-3-4) 729–961 CE, compared to the age of the whole bulk of this sample and the charcoal, both falling into the interval 644–765 CE. ff = binder fine fraction, LL = lime lumps.

https://doi.org/10.1017/RDC.2020.35 Published online by Cambridge University Press

(with the binder dating giving a slightly older age due to the residual presence of dead carbon). From this, it can be assumed that the speed of acid hydrolysis of residual dolomite was not always significantly slower than the hydrolysis of the calcite binder. Indeed, the solubility of dolomite is depending on the Mg content and the order of the molecules (Railsback 2006). The dolomite rocks in the Val Müstair show a high variability both of the size of the crystals and of the texture (Cavallo et al. 2019) and therefore it cannot be excluded that some of them were already dissolved in the first fractions of the sequential dissolution. It can be said, however, that the treatment has rejuvenated the results by converging towards a correct value, but further refinement of the technique of sample preparation for eliminating dolomitic sand residue is necessary for achieving fully reliable results.

Finally, the presence of a plateau in the calibration curve in the range between 700 and 900 CE results in a wider uncertainty on the dating of the Carolingian phase than for other historical periods.

CONCLUSION

This preliminary study demonstrates that ^{14}C dating with sequential dissolution has a potential for dating the mortars of Müstair, made from dolomitic raw material even if the dolomite presence complicates the situation. The results obtained for the main church samples are in agreement with its dendrochronological dating, but when a contamination from fine dolomitic aggregate is present further investigation is required to develop a more adequate sample preparation technique. This case has confirmed that for dating dolomitic mortar, lime lumps and 45–63 μm sieved fractions are complementary materials for a reliable mortar dating, while significant differences emerge in using the bulk. The dating of 63–75 μm sieved fractions or even the bulk of lime lumps can result in spurious ages.

ACKNOWLEDGMENTS

The authors thank the anonymous reviewers for suggestions and comments. The authors would like to acknowledge Christine Bläuer for the helpful suggestions that improved the text. Special thanks go to the Department of Chemical and Geological Sciences of the University of Modena and Reggio Emilia and in particular Dr. Simona Marchetti Dori under the scientific direction of Dr. Francesco Ronchetti for the preparation of thin sections and Prof. Alessandro Gualtieri for XRPD analyses. This project has been made possible thanks to the financial support provided by SNSF (Swiss National Science Foundation, Switzerland – Grant project number 105211_169411) and Biosfera Val Müstair (https://www.biosfera.ch/de).

REFERENCES

Altomare A, Corriero N, Cuocci C, Falcicchio A, Moliterni A, Rizzi R. 2015. QualX2.0: a qualitative phase analysis software using the freely available database POW_COD. Journal of Applied Crystallography 48:598–603.

Caroselli M, Bläuer C, Cassitti P, Cavallo G, Hajdas I, Hueglin S, Neukom H, Jornet A. 2019. Insights into Carolingian construction techniques – results from archaeological and mineralogical studies at Müstair Monastery, Grisons, Switzerland. Proceedings of the 5th Historic Mortars Conference – HMC2019:743–757.

Cavallo G, Caroselli M, Jornet A, Cassitti P. 2019. Preliminary research on potential raw material sources for dolomitic lime mortars at St. John's convent at Müstair, Switzerland. Proceedings of the 5th Historic Mortars Conference – HMC2019:628–641.

Descoeudres G. 2007. Herrenhäuser aus Holz. Eine mittelalterliche Wohnbaugruppe in der

https://doi.org/10.1017/RDC.2020.35 Published online by Cambridge University Press

Innerschweiz. Schweizer Beiträge zur Kulturgeschichte und Archäologie des Mittelalters, Bd. 34. Schweizerischer Burgenverein, Basel.

Diekamp A, Konzett J, Mirwald PW. 2009. Magnesian lime mortars—identification of magnesiumphases in medieval mortars and plasters with imaging techniques. In: Middendorf B, Just A, Klein D, Glaubitt A, Simon J, editors. Proceedings of the 12th Euroseminar on Microscopy Applied to Building Materials, 15–19.09.2009. Dortmund, Germany:309–17.

Elsen J. 2006. Microscopy of historic mortars—a review. Cement and Concrete Research 36(8): 1416–1424.

Folk RL, Valastro S. 1976. Successful technique for dating of lime mortar by carbon-14. Journal of Field Archaeology 3(2):195–201.

Goll J, Exner M, Hirsch S. 2007. Müstair. Die mittelalterlichen Wandbilder in der Klosterkirche. Zürich: Verlag Neue Zürcher Zeitung.

Grabherr G. 2006. Die Via Claudia Augusta in Nordtirol – Methode, Verlauf, Funde. In: Walde E, Grabherr G, editors. Via Claudia Augusta und Römerstraßenforschung im östlichen Alpenraum. Ikarus 1. Innsbruck: Innsbruck University Press. p. 36–336.

Gražulis S, Chateigner D, Downs RT, Yokochi AF, Qiurós M, Lutterotti L, Manakova E, Butkus J, Moeck P, Le Bail A. 2009. Crystallography Open Database – an open-access collection of crystal structures. Journal of Applied Crystallography 42(4):726–729.

Hajdas I, Trumm J, Bonani G, Biechele C, Maurer M, Wacker L. 2012. Roman ruins as an experiment for radiocarbon dating of mortar. Radiocarbon 54(3–4):897–903.

Hajdas I, Lindroos A, Heinemeier J, Ringbom Å, Marzaioli F, Terrasi F, Passariello I, Capano M, Artioli G, Addis A, Secco M, Michalska D, Czernik J, Goslar T, Hayen R, Van Strydonck M, Fontaine L, Boudin M, Maspero F, Panzeri L, Galli A, Urbanova P, Guibert P. 2017. Preparation and dating of mortar samples –Mortar Dating Inter-Comparison Study (MODIS). Radiocarbon 59(6):1845–1858.

Hajdas I, Maurer M, Röttig MB. 2020. Development of ^{14}C dating of mortars at ETH Zurich. Radiocarbon 62. This issue.

Heinemeier J, Ringbom A, Lindroos A, Sveinbjornsdottir AE. 2010. Successful AMS ^{14}C dating of non-hydraulic lime mortars from the Medieval churches of the Aland Islands, Finland. Radiocarbon 52:171–204.

Hodges R. 1993. San Vincenzo al Volturno 1, Archaeological Monographies of the British School at Rome 7. London: British School at Rome.

Hurni JP, Orcel C, Tercier J. 2007. Zu den dendrochronologischen Untersuchungen von Hölzern aus St. Johann in Müstair. In: Sennhauser HR, editor. Müstair Kloster St. Johann 4. Naturwissenschaftliche und technische Beiträge. Zürich: vdf Hochschulverlag. p. 99–116.

Lindroos A, Heinemeier J, Ringbom Å, Braskén M, Sveinbjörnsdóttir Á. 2007. Mortar dating using AMS ^{14}C and sequential dissolution: examples from medieval, non-hydraulic lime mortars from the Åland Islands, SW Finland. Radiocarbon 49(1):47–67.

Lindroos A, Ringbom Å, Heinemeier J, Hodgins G, Sonck-Koota P, Sjöberg P, Lancaster L, Kaisti R, Brock F, Ranta H, Caroselli M, Lugli S. 2018. Radiocarbon dating historical mortars: lime lumps or/and binder carbonate? Radiocarbon 60(3):875–899.

Lubritto C, Caroselli M, Lugli S, Marzaioli F, Nonni S, Marchetti Dori S, Terrasi F. 2015. AMS radiocarbon dating of mortar: The case study of the medieval UNESCO site of Modena. Nuclear Instruments and Methods in Physics Research B 361:614–619.

Michalska D, Czernik J, Gosar T. 2017. Methodological aspect of mortars dating (Poznań, Poland, MODIS). Radiocarbon 59(6): 1891–1906.

Railsback LB. 2006. Solubility of common carbonate minerals. In: Some fundamentals of mineralogy and geochemistry. Online book. Available at www.gly.uga.edu/railsback.

Ramsey CB, Lee S. 2013. Recent and planned developments of the program OxCal. Radiocarbon 55:720–730.

Reimer PJ, Bard E, Bayliss A, Beck JW, Blackwell PG, Ramsey CB, Buck CE, Cheng H, Edwards RL, Friedrich M, Grootes PM, Guilderson TP, Haflidason H, Hajdas I, Hatte C, Heaton TJ, Hoffmann DL, Hogg AG, Hughen KA, Kaiser KF, Kromer B, Manning SW, Niu M, Reimer RW, Richards DA, Scott EM, Southon JR, Staff RA, Turney CSM, and van der Plicht J. 2013. IntCal13 and Marine13 radiocarbon age calibration curves 0–50,000 years cal BP. Radiocarbon 55:1869–1887.

Ruff M, Szidat S, Gaggeler HW, Suter M, Synal HA, Wacker L. 2010. Gaseous radiocarbon measurements of small samples. Nuclear Instruments and Methods in Physics Research B 268:790–794.

Sennhauser HR, Courvoisier HR. 1996. Die Klosterbauten – eine Übersicht. In: Sennhauser HR, editor. Müstair, Kloster St. Johann. Bd. 1: Zur Klosteranlage. Vorklösterliche Befunde. Vdf, Zürich. p. 15–65.

https://doi.org/10.1017/RDC.2020.35 Published online by Cambridge University Press

Stuiver M, Polach HA. 1977. Discussion: Reporting of ^{14}C data. Radiocarbon 19(3):355–363.

Synal HA, Stocker M, Suter M. 2007. MICADAS: A new compact radiocarbon AMS system. Nuclear Instruments and Methods in Physics Research B 259:7–13.

Wacker L, Güttler D, Goll J, Hurni JP, Synal HA, Walti N. 2014. Radiocarbon dating to a single year by means of rapid atmospheric ^{14}C changes. Radiocarbon 56(2):73–579.

Warren J. 2000. Dolomite: occurrence, evolution and economically important associations. Earth-Science Reviews 52(1–3):1–81.

Zettler A. 1988. Die frühen Klosterbauten der Reichenau. Thorbecke, Sigmaringen.

https://doi.org/10.1017/RDC.2020.35 Published online by Cambridge University Press